Cytometry 6:13–21 (1985)

Two-Dimensional Impedance Studies of BSA Buoyant Density Separated Human Erythrocytes

R.C. Leif, S. Schwartz, C.M. Rodriguez, L. Pell-Fernandez, M. Groves, S.B. Leif, M. Cayer, and H. Crews

Coulter Electronics, Inc., Hialeah, Florida 33010 (R.C.L., C.M.R., L.P.-F., M.G., S.B.L., H.C.), Papanicolau Cancer Research Institute (R.C.L., M.C.) and Department of Biomedical Engineering, University of Miami (R.C.L., S.S.), Miami, Florida 33124

Received for publication June 1, 1983; accepted May 24, 1984

Combined DC (Coulter Volume) and radio frequency impedance studies were performed on human erythrocytes which had been separated by buoyant density in linear, neutral, isotonic bovine serum albumin gradients. The individual buoyant density fractions showed no reproducible shift in volume with buoyant density but did show a shift with opacity, radio frequency impedance divided by dc impedance. This new electronic parameter of opacity can be related to cell age, since both it and cell age are directly related to buoyant density. This increase in opacity with buoyant density is correlated with a change in shape.

Key terms: **Coulter electronic cell volume, opacity, erythrocytes, impedance, radio frequency, buoyant density, bovine serum albumin (BSA), density gradient centrifugation**

Leif and co-workers (9,13) proposed that automated cell analysis should be based on the assumption that there are many descriptors available that permit the easy identification of each type of cell present in a heterodisperse population. However, the use of a combination of two impedance measurements (13,5) together with multidimensional fluorescence and light scattering data on a cell-by-cell basis should allow adequate quantification of cellular parameters for specific identification of cells. For flow analysis to maintain a high level of accuracy, it will be necessary to include redundant information by increasing the dimensionality of data in order to prevent errors.

The Coulter volume measurement, which was one of the first parameters to be used for the automated counting and analysis of biological cells (2,3), is an impedance measurement at zero frequency (dc) or a measure of resistance. Besides the abovementioned dc resistance (electronic cell volume) measurements, it is possible to perform simultaneously ac impedance measurements. An instrument for this purpose has been developed by Coulter and Hogg (4). The highest resolution in a two-dimensional distribution is achieved by producing orthogonal parameters. In the present case, this was accomplished by dividing the radio frequency ac impedance by the dc resistance, which is defined as the opacity.

Hoffman and Britt (6) developed a flow-system technique that simultaneously detected the dc Coulter volume and ac impedance. As pointed out by the authors, the use of the low ac frequency of 1 MHz resulted in "a high correlation between the ac and dc parameters for CHO cells." These authors performed their measurements at the reactance maximum in order to maximize the difference between cell types (Britt, personal communication) rather than at the higher frequency range. The ac impedance changes slowly with frequency above approximately 20 MHz, where, according to the bulk measurements of erythrocyte suspensions by Jenin et al. (7), the conductance of intact erythrocytes plateaus. According to these authors, the erythrocyte membrane appears to be practically short-circuited at frequencies above 50 MHz.

The purpose of this study was to determine the relationship of the electrical parameters of Coulter volume and opacity to erythrocyte buoyant density. It was demonstrated previously that buoyant density, as determined in linear gradients of bovine serum albumin, was directly related to rabbit erythrocyte age (8,10). Thus, a relationship between impedance measurements and buoyant density should also correlate with erythrocyte age. If the relationship between opacity and buoyant density demonstrated in this study holds for other classes of cells, then, since buoyant density is related to stage of differentiation (12,19), it should be possible to determine population shifts and even leukemic or other cancer cells in blood or other cell samples that are at present

Address reprint requests to R.C. Leif, Coulter Electronics, Inc., Applied Research, 690 W. 20th Street, Hialeah, FL 33010.

manually analyzed on a slide. The findings of Leif and Vinograd (8,10) that the shift of the erythrocyte volume distribution with buoyant density was minimal were also tested in this study.

MATERIALS AND METHODS

Blood was obtained from two donors, one female aged 23 and one male aged 38, both of apparently normal health. Approximately 0.5 mL of human blood obtained by finger puncture was added to a 2-mL disposable Autoanalyzer cuvette (ElKay Products, Inc.; Worchester, MA) which contains 1.0 mL of counting medium (Table 1) and a few grains of Chelex (Bio-Rad, Laboratories; Richmond, CA).

After the blood was dispersed, the Chelex grains were allowed to sediment for approximately 30 s and the cell suspension was decanted into a test tube. The test tube was centrifuged for 1 min using a force of 200 g, and the supernatant was aspirated. The pellet was suspended in 0.5 mL of viscous solution which prevents centrifugation artifacts (11). This solution is prepared by dissolving 0.05 g Sigma herring sperm DNA in 1.0 mL of 199B (Table 1). A linear, isotonic, and neutral BSA gradient was formed with the gradient system described by Leif (14). The composition of the BSA solution is listed in Table 1. This gradient system consists of special centrifuge tubes, a gradient mixing chamber, a double-sided undulating diaphragm peristaltic pump, a digital controller, and a cold bench. A plastic floating washer was placed on top of the gradient column. Then the erythrocyte suspension was carefully placed inside of this washer by means of two 200-μL aliquots delivered by an adjustable volume pipetting device (Rainen Pipetman 0-200 fL; Woburn, MA) equipped with disposable tips. Centrifugation was for 1 h at 10,000 g using an SW25 rotor in a Beckman L2-65B ultracentrifuge utilizing a manual acceleration control as described by Leif (14). Fractions were then pumped out of the special centrifuge tubes and at the end of each isovolumic pumping cycle, collected manually, into Polyvials (2 dram; Olympic Plastics; Los Angeles, CA).

The refractive index of each fraction was determined with a Bausch & Lomb refractometer. These values were converted to density units with the relation given by Leif (14): N^D_{25} (1.580) − 1.109 = ρ(BSA) where N^D_{25} = refractive index at 25°C and ρ(BSA) = density of the BSA solution.

The fractions were packed in ice in a lucite carrier designed to facilitate their transport (14). Measurements began 1 h later finishing in approximately 3 h. 0.50 mL of each gradient fraction was diluted with 5 mL of Iso C® (Coulter Electronics, Inc., Hialeah, FL) which contained 0.3% BSA. Polystyrene latex microspheres, 5.13 μm diameter (Coulter Electronics, Inc., Hialeah, FL) in Iso C, served as an internal standard. All Iso C with BSA solutions were filtered with an Acrodisc disposable filter assembly (0.2 μm, Gelman) before addition of spheres and cells. The individual fractions were counted on a COULTER COUNTER® Model ZBI. The average recovery rate of the cells from the gradients was 68%. The recovery would have been significantly increased had the cells which had sedimented to the bottom of the special centrifuge tube been recovered.

The electronic measurements were performed with a laminar flow Coulter multifrequency apparatus (4). The aperture was 50 μm in diameter and 60 μm long. The dc current was 0.5 mA and the ac frequency was 34 MHz, which is well within the conductivity plateau region of the erythrocyte impedance according to Jenin et al. (7). Decreasing the frequency to 23 MHz produced similar results to those presented in this study, and thus it was further established that the measurements described below were in the plateau region.

The scattergrams of the two-dimensional dc impedance and opacity distributions were obtained by photographing the individual analog data points, which were shown on a standard Tektronix Model 603 oscilloscope. The optimum film was Polaroid Type 611 Video Image

Table 1
Composition of Salt Solutions and BSA Media

Substance	BSA-199L(CO_2) (g/kg BSA)	199(B) (g/liter)	LP-0.2 BSA (g/liter)	Counting medium (g/liter)
Medium 199 with glutamine but without salts or glucose	0.546	0.820		
$NaHCO_3$		2.200		
Na_2CO_3	3.350			
$NaH_2PO_4 \cdot H_2O$	0.184	0.276	0.276	0.040
$Na_2HPO_4 \cdot 7H_2O$			1.755	0.225
NaCl	1.929	6.903	6.903	7.586
NaF				0.500
KCl	0.225	0.337	0.337	0.337
$MgSO_4 \cdot 7H_2O$	0.142	0.213	0.213	
$CaCl_2$	0.082	0.123	0.123	
Glucose	0.667	1.000	1.000	
BSA (33% deionized)			6.06	
Neomycin sulfate	0.089		0.100	

Recording Black and White because it showed intermediate shades which are a result of superimposed data points. The pulse-height analyses of both dc impedance and opacity were separately performed with a Coulter Channelyzer® instrument and plotted out with a Coulter XY Recorder. For most experiments the opacity pulse-height data was stored in digital form with a Coulter M3 Data Converter.

ANALYSIS OF DATA

The data describing the BSA gradients was analyzed as described by Leif (14). The resulting data was graphed with a Hewlett-Packard four-color plotter. The calculated buoyant density was determined as described previously (10) by plotting the individual densities determined from the refractive indices and interpolating the values from the straight line plotted through the individual points. The normalized buoyant density distribution, $F(\rho)$, which is the number of cells per fraction divided by the product of the total number of cells recovered from the gradient and the density range per fraction, was plotted against the buoyant density of the individual fractions.

All electronic opacity values were normalized to the median of the sphere distribution, which is given as 100% normalized opacity, henceforth referred to as 100 opacity units. The accuracy of the red blood cell opacity distributions was significantly enhanced by the use of a reference standard consisting of a dilute suspension of 71 μm^3 polystyrene latex spheres (standard deviation of 0.3 opacity units) as an internal standard to compensate for any drift of the apparatus that may have occurred.

Because of the lack of knowledge of both the shape and the width of the erythrocyte volume distribution and the fact that a reference channel had to be obtained from the pulse-height analysis, it was necessary to employ the midpoint function (8,10). The midpoint function is calculated by summing the interpolated values of the abscissa at given percentages of the ordinate maximum (in steps of 10 starting at 20) and dividing by the number of interpolated values, in this case 18. The amplitude of the dc amplifier was always adjusted to place the mode of the sphere distribution on channel 71 in accordance with their true volume being 71 μm^3. The midpoint function was also employed for the erythrocyte opacity distribution except, as stated above, it had to be normalized in terms of the internal standard.

RESULTS

Electrical measurements to demonstrate short-term stability were performed on a sample of whole blood, obtained by finger prick from the female, and stored for approximately 2 h in ice. The values obtained from three measurements which were performed over short periods of time (i.e., 17 min) are given in Table 2. It demonstrates that no significant drift occurred in either equivalent sphere Coulter volume or opacity during this time interval.

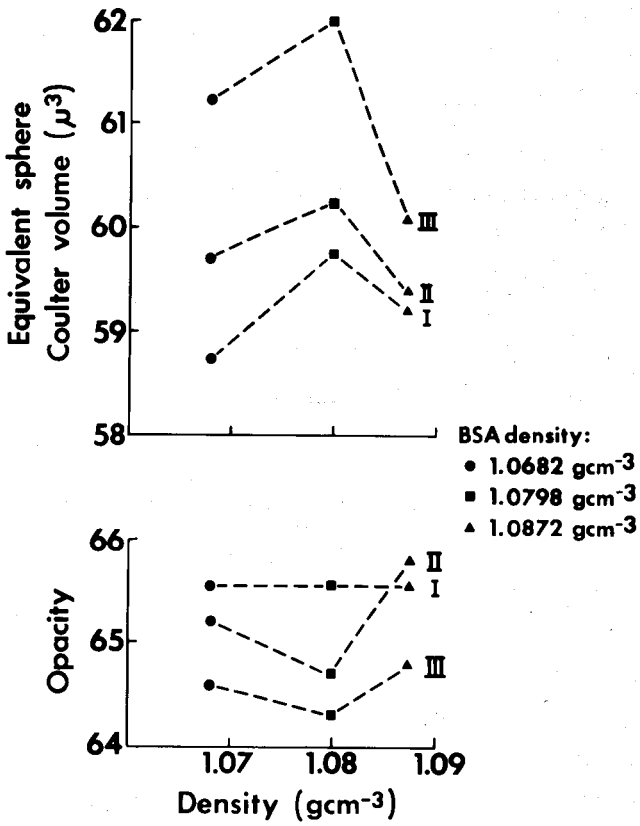

FIG. 1. Equivalent sphere Coulter volume (top) and opacity (bottom) plotted against BSA density in control experiments to determine the effect of time in BSA. Roman numerals indicate order in which measurements were recorded. Experiment I is considered time 0 (actually, 15 min after finger prick), experiment II was recorded approximately 140 min later, and experiment III was recorded approximately 91 min after II.

Table 2
Reproducibility Study

	125[a]	135[a]	142[a]	Average
Opacity	61.7	61.4	61.4	61.5 ± 0.22
% CV	4.96	4.92	5.08	4.99 ± 0.09
Equivalent sphere Coulter volume	63.3	63.4	63.4	63.4 ± 0.06
% CV	11.63	12.21	11.55	11.80 ± 0.41

[a]Time in minutes.

The effect of gradient materials on the measurement was determined by adjusting the refractive indices to give three erythrocyte-containing-BSA suspensions with BSA densities corresponding to the light, middle, and dense portions of a true gradient (1.0682, 1.0798, and 1.0872 gcm^{-3}, respectively). Electrical measurements, performed on the three fractions consecutively, began 15 min after the finger puncture and were repeated twice within a period of approximately 300 min (Fig.1), which corresponded to the total period of a typical experiment. No clear trend or significant change in either Coulter volume or opacity due to the effect of BSA concentration is evident.

Table 3
Buoyant Density Midpoints

Experiment date		
♀ 08-08-79	1.0781	
♀ 10-19-79	1.0786	
♀ 12-28-79	1.0830	
♀ 01-04-80	1.0799	Av = 1.0799; S.D. = .0022
♂ 08-15-79	1.0808	
♂ 02-01-80	1.0813	Av = 1.0811

Studies of Buoyant Density Separated Cells

Four density gradient experiments over a period of 6 months were performed on the blood from the female and two on the blood from the male donor over a 7-month span. A composite of oscilloscope photos showing the individual two-dimensional scattergrams obtained from each of the individual fractions of a gradient performed on the male subject (Fig. 2) visually illustrates

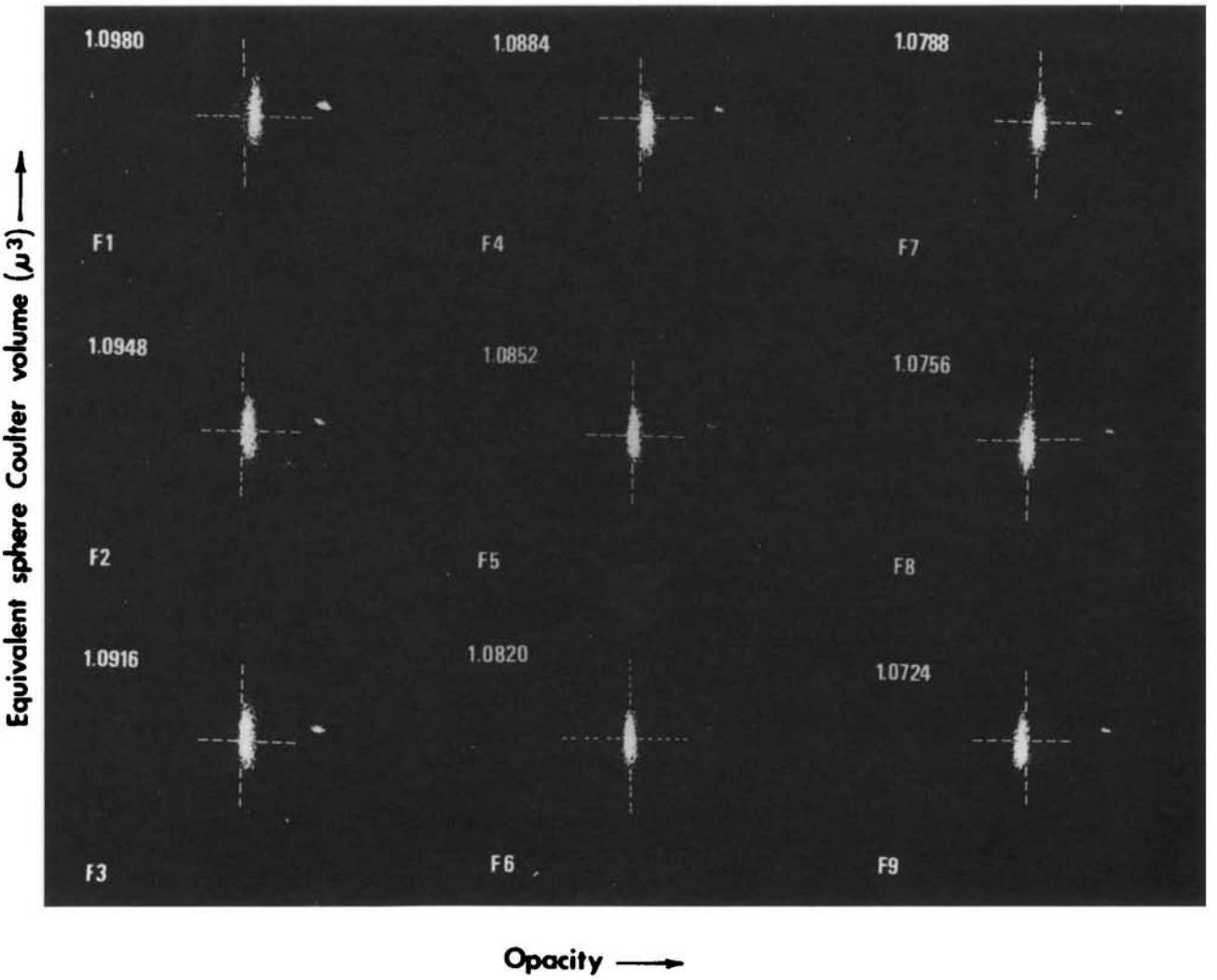

FIG. 2. Two-dimensional scattergrams of volume vs opacity of cells from a gradient. The dotted lines are reference axes indicating shifts in the erythrocyte scattergrams relative to that of fraction 6 which has density closest to that of the average for the male RBC (i.e., 1.0811 gcm^{-3}). As in all of the following experiments, the polystyrene latex spheres are employed as a constant reference of 71 μm^3 and 100 opacity units.

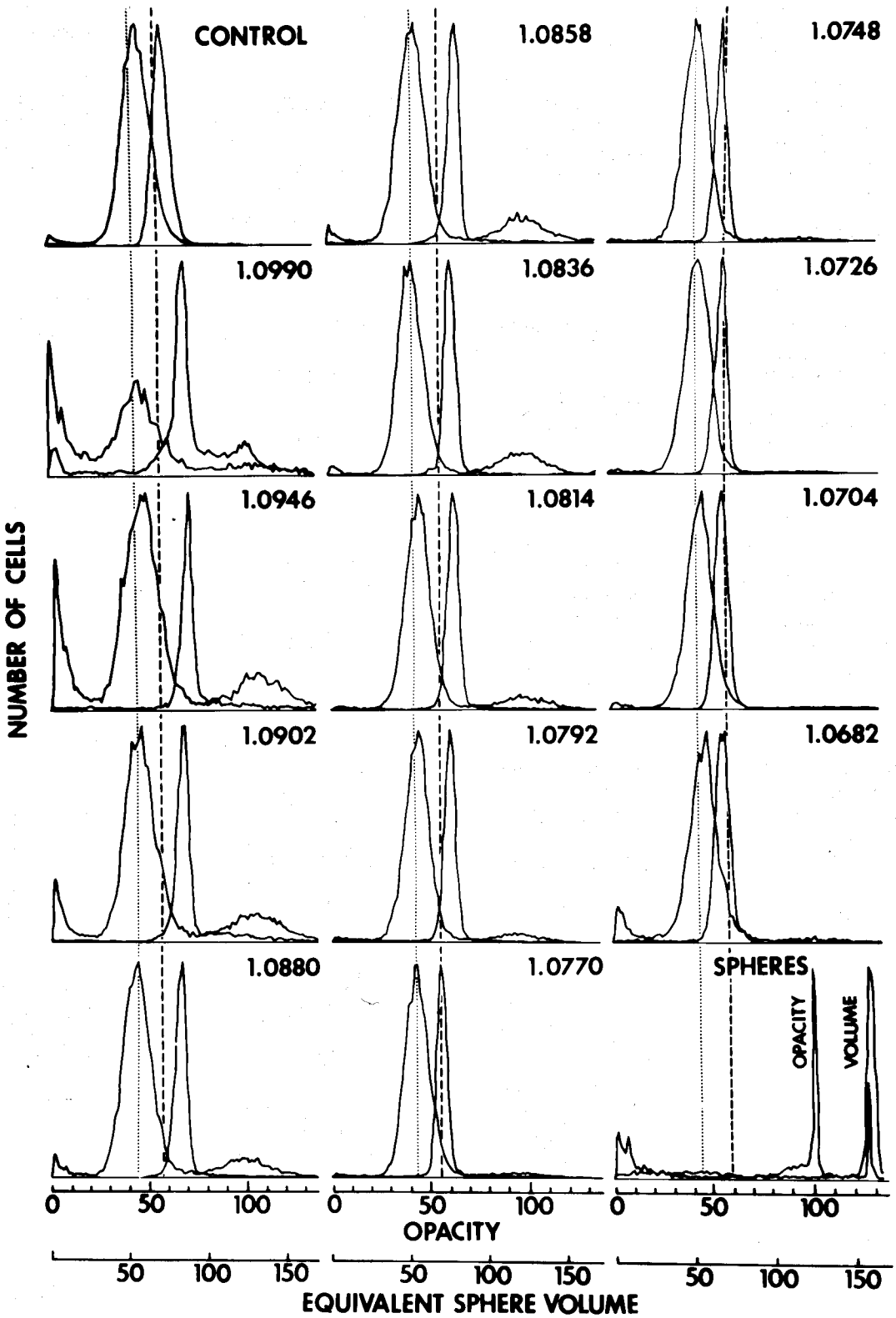

FIG. 3. Single-dimensional pulse-height histograms of both the electronic cell volume and opacity distributions of the individual buoyant density fractions and the control distribution. The wider distributions, shown on the left of each plot, are the electronic cell volumes. The narrower distributions, shown on the right of each plot, are the opacities. The results for the calibrating spheres are shown to the lower right. The vertical lines correspond to the midpoint of the volume and the truncated median of the opacity of the midpoint fraction of the buoyant density distribution (density = 1.0770 gcm^{-3}).

the shift of opacity distribution with changing density. There appear to be no discernible differences or shifts with respect to the equivalent sphere Coulter volume. Scattergrams from other density separations showed essentially similar results. The single-parameter pulse-height analyses of the individual density fractions obtained on a gradient performed a year previous to this study on the same subject demonstrated similar results (Fig. 3).

In order to demonstrate that erythrocyte opacity is related to buoyant density, two gradient fractions, 3 and 9 (1.0916 gcm^{-3} and 1.0724 gcm^{-3}, respectively) of separated male human cells were combined and then analyzed electronically. Figure 4 shows the resulting one-parameter opacity pulse-height analysis distributions. The opacity of the more dense fraction 3 is 64.6 units and that of the less dense fraction 9 is 59.2 units. Both are unimodal in opacity as are all fractions observed to date. The opacity distribution of the mixture, however, exhibits two peaks. The apparatus was therefore measuring the opacity of two distinct subpopulations, and the pulse-height differences are real and not due to drift of either the cells or apparatus.

Data from an individual experiment (Fig. 5) illustrated the trends with buoyant density of the individual midpoints of the opacity and equivalent sphere Coulter volume distributions of the buoyant density fractions. The normalized buoyant density distribution function, $F(\rho)$ the fraction of cells per density interval, was highly reproducible, with an average midpoint of 1.0799 gcm^{-3}, a standard deviation of $\pm$ 0.0022 (Table 3) and range of 0.0049 gcm^{-3}, for cells from the female subject and the average midpoint for cells from the male was 1.0811 gcm^{-3}, from two experiments having average $F(\rho)$'s of 1.0808 and 1.0813 gcm^{-3}.

In a typical gradient separation of female blood cells (Fig. 5) the opacity increased from 59.1 to 63.9 units (i.e., 8%) over a density range of 1.076 to 1.089 gcm^{-3}. The correlation of the equivalent sphere Coulter volume with buoyant density cannot be accurately quantified since the error for the individual determinations is evidently greater than the excursion of the data points. Thus, there is no apparent correlation. The other three gradients for the female revealed very similar results.

The averaged values of the opacity, equivalent sphere Coulter volume, and $F(\rho)$ were plotted against buoyant density (Fig. 6a–c). The averages were determined and aligned by the procedure described in earlier work (8,10).

The data obtained using blood from the male donor appeared similar to those of the female except for a broader distribution of $F(\rho)$. The opacity increased from 61.3 to 69.7 units spanning a density range from 1.0731 gcm^{-3} to 1.0941 gcm^{-3}. The equivalent sphere Coulter volume also showed no consistent trend with density.

Averaged curves of cells from the male subject appeared similar to those of the female. Since there were only two sets of data, no standard deviation was computed.

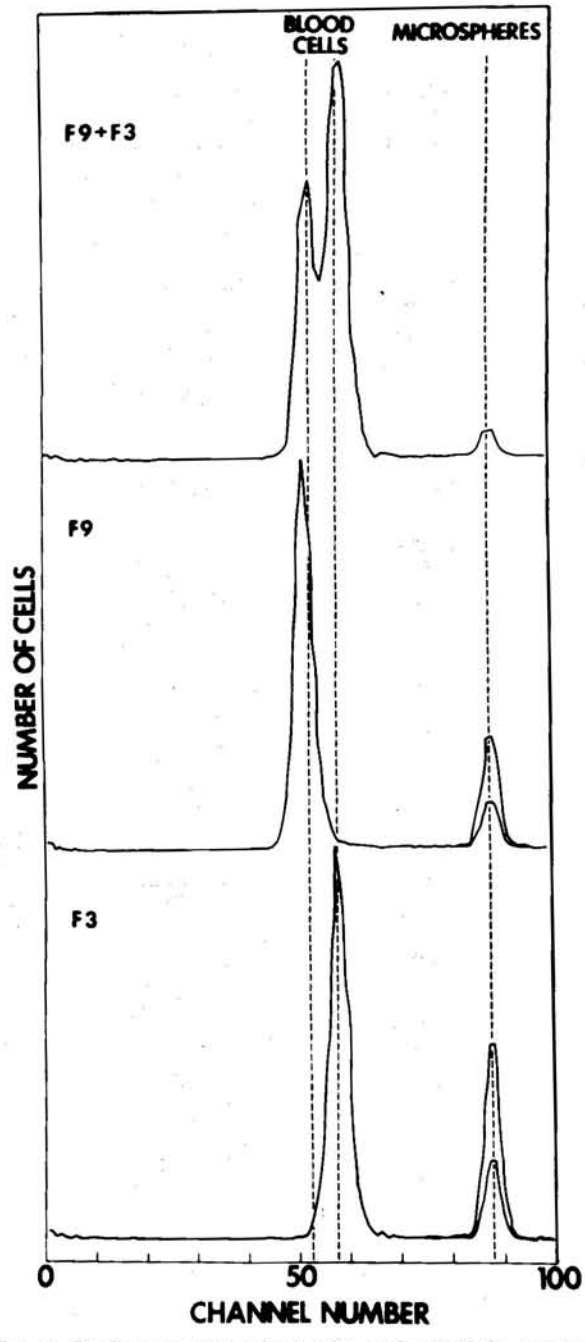

FIG. 4. Single-parameter pulse-height analyses of the opacity of buoyant density fraction 3 (bottom), fraction 9 (middle), and fractions 3 and 9 combined (top) obtained from a gradient of cells from the male subject. Left peaks are erythrocytes and right peaks are microspheres.

In general, the average opacity of the individual gradient fractions increased with increasing buoyant density except for the first few lighter density fractions. All equivalent sphere Coulter volume curves showed enough inconsistencies from one gradient to the next that no common trend could be determined. The $F(\rho)$'s all had

basically the same shape, varying slightly in terms of midpoint and peak value.

CONCLUSIONS

Erythrocyte opacity shows a clear increase with increasing buoyant density at all except the least dense end of the distribution which is contaminated with both reticulocytes and leukocytes. If a trend relating buoyant density and Coulter volume does exist it is much less of a correlation than that which exists with opacity. This is in agreement with previous results (8). Interestingly, the volume distributions of the density fractions and controls have apparently the same shape and breadth as demonstrated by their coefficients of variation and overlap.

It should be cautioned that all of our volume measurements are equivalent sphere volumes. It was demonstrated by Leif and Vinograd (8) and Leif (10) that there is a significant change in shape of the erythrocyte, and differences in deformability have been reported by Mel and Yee (15) and by Schmid-Schonbeim and Gaehtgeus (18). It is therefore quite possible that the effect of changes in shape could cancel or at least partially mask a true volume change. In fact all of the previous separation studies involved larger orifices and thus would have produced results less affected by erythrocyte deformability (M. Groves, unpublished results). Thus the shape factor differences could have cancelled out any small shifts in cell volume.

A decrease in electronic cell volume and concomitant increase of mean cellular hemoglobin concentration with density have been observed in other studies. However, those studies either involved other gradient media such as Percoll with 5% BSA (17), or high-speed centrifugation 39,000 g at 30°C for 1 h (1), reported average buoyant density greater than that observed with BSA, and did not report an equivalent separation by age. Leif and Vinograd (8) did find a decrease in cellular volume with buoyant density but did not find any significant change in mean cellular hemoglobin concentration across the gradient.

The results in the case of opacity are definitive. Buoyant density separation in linear BSA gradients clearly divides the continuous opacity distribution into subpopulations. In regard to opacity, except for the light end of the distribution where contamination by reticulocytes and leukocytes exists, the opacity shows a clear increase with increasing buoyant density. This relationship was

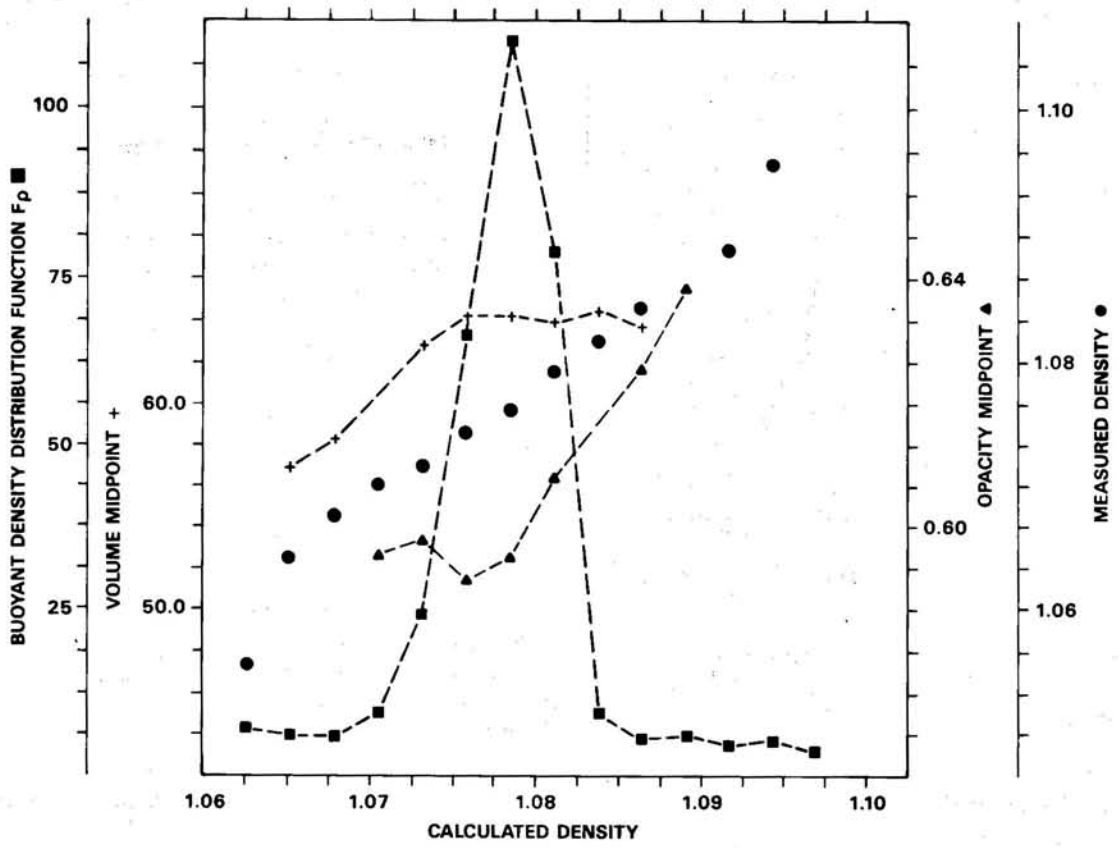

FIG. 5. Buoyant density distribution F(ρ), measured density, midpoint of the single-parameter pulse-height distributions of opacity, and equivalent sphere Coulter volume plotted against calculated density of cells from the female subject. Although there is no discernable trend in the volume distributions, the points have been connected to facilitate visualization. The calculated densities were read off a straight line fitted to the measured densities. The left outside ordinate is the buoyant density distribution function, the left inside ordinate is the volume midpoint. The right inside ordinate is the opacity midpoint. The right outside ordinate is the measured density.

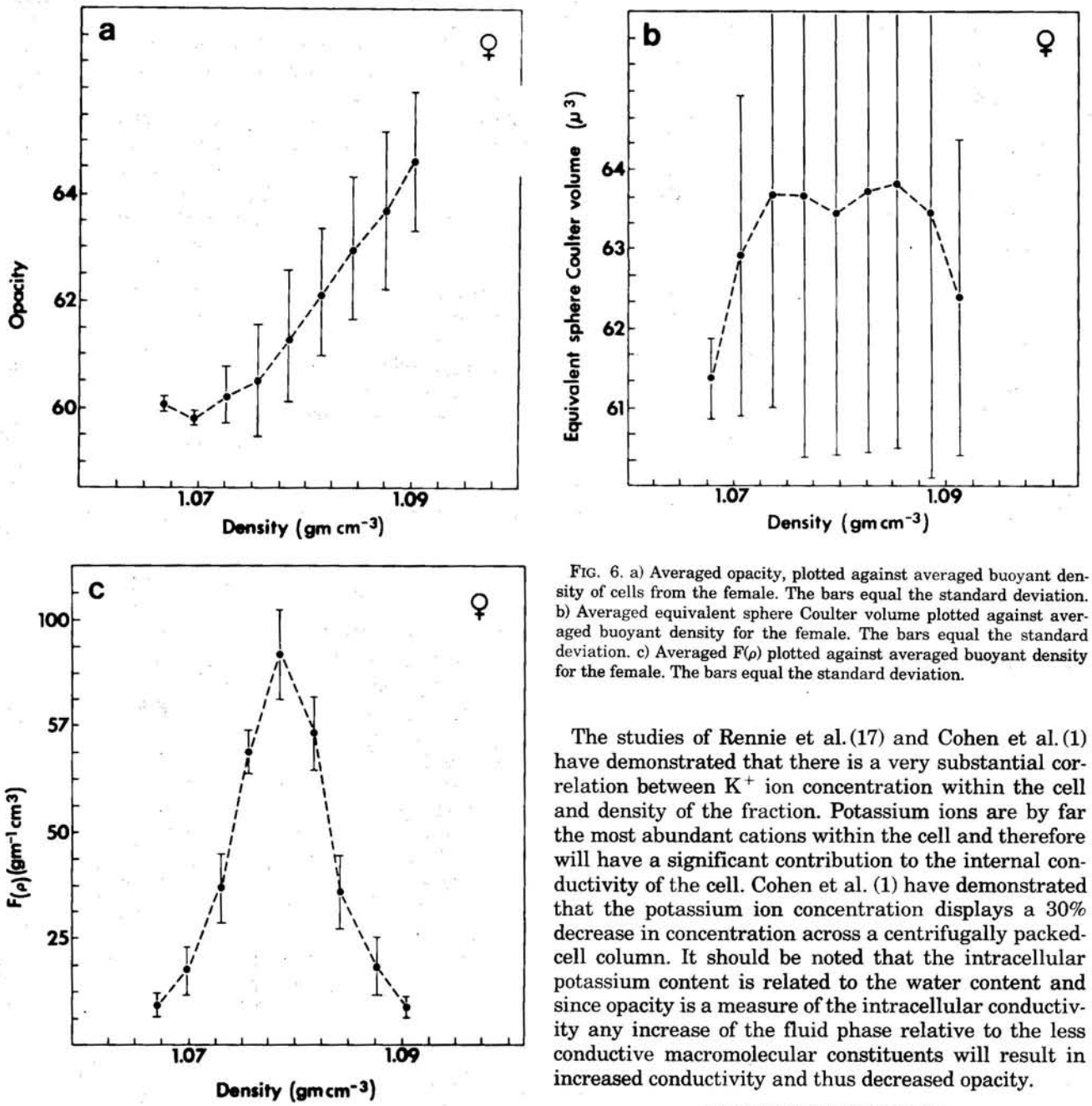

FIG. 6. a) Averaged opacity, plotted against averaged buoyant density of cells from the female. The bars equal the standard deviation. b) Averaged equivalent sphere Coulter volume plotted against averaged buoyant density for the female. The bars equal the standard deviation. c) Averaged $F(\rho)$ plotted against averaged buoyant density for the female. The bars equal the standard deviation.

evident in all of the two-parameter impedance studies of buoyant density gradient separations, male and female, and was particularly obvious in the averaged curves of those measurements.

Previously, it has been demonstrated that buoyant density, as determined in linear gradients of bovine serum albumin, was directly related to rabbit erythrocyte age (8,16). Having demonstrated that opacity increases with increasing buoyant density, and since buoyant density is directly related to erythrocyte age, opacity is thus directly related to erythrocyte age.

The studies of Rennie et al. (17) and Cohen et al. (1) have demonstrated that there is a very substantial correlation between K^+ ion concentration within the cell and density of the fraction. Potassium ions are by far the most abundant cations within the cell and therefore will have a significant contribution to the internal conductivity of the cell. Cohen et al. (1) have demonstrated that the potassium ion concentration displays a 30% decrease in concentration across a centrifugally packed-cell column. It should be noted that the intracellular potassium content is related to the water content and since opacity is a measure of the intracellular conductivity any increase of the fluid phase relative to the less conductive macromolecular constituents will result in increased conductivity and thus decreased opacity.

ACKNOWLEDGMENTS

We wish to thank W.H. Coulter and W. Hogg for kindly making available their two-parameter impedance system for these studies and Coulter Electronics, Inc., for supporting this basic research in cell biology. We wish to dedicate this paper to the memory of Walter Hogg.

LITERATURE CITED

1. Cohen NS, Ekholm JE, Luthra MG, Hanahan J: Biochemical characterization of density-separated human erythrocytes. Biochim Biophys Acta 419:229–242, 1976.
2. Coulter WH: Means for Counting Particles Suspended in a Fluid. US Patent 2,656,508, 1953.

3. Coulter WH: High speed automatic blood cell counter and cell size analyzer. Proc Natl Electron Conf 12:1034–1042, 1956.
4. Coulter WH, Hogg WR: Signal modulated apparatus for generating and detecting resistance and reactive changes in a modulated current passed for particle classification and analysis. US Patent 3,502,974, 1970.
5. Groves MR: Application of the electrical sizing principle of Coulter to a new multiparameter system. IEEE Trans Biomed Eng V:BME-27, 1980.
6. Hoffman RA, Britt WB: Flow-system measurement of cell impedance properties. J Histochem Cytochem 27:234–240, 1978.
7. Jenin PC, Schwan HP: Some observations on the dielectric properties of hemoglobin's suspending medium inside human erythrocytes. Biophys J 30:283–293, 1980.
8. Leif RC, Vinograd J: The distribution of buoyant density of human erythrocytes in bovine albumin solutions. Proc Natl Acad Sci USA 51:520–528, 1964.
9. Leif RC: A Proposal for an Automated Multiparameter Analyzer for Cells (AMAC). In: Automated Cell Identification and Sorting, Wied GL, Bahr GF (eds). Academic Press, New York, 1970, pp 131–159.
10. Leif RC: Buoyant density separation of cells. In: Automated Cell Indentification and Sorting, Wied GL, Bahr GF (eds). Academic Press, New York, 1970, pp 21–96.
11. Leif RC, Kneece WC Jr, Warters RL, Grinvalsky H, Thomas RA: Density Gradient System III. Elimination of hydrodynamic, wall, and swirling artifacts in preformed isopycnic gradient centrifugation. Anal Biochem 45:357–373, 1972.
12. Leif RC, Smith S, Warters RL, Dunlap LA, Leif SB: The buoyant density distribution of guinea pig bone marrow cells. J Histochem Cytochem 23:378–389, 1975.
13. Leif RC, Thomas RA, Yopp TA, Watson BD, Guarino VR, Hindman DHK, Lefkove N, Vallarino LM: Development instrumentation and fluorochromes for automated multiparameter analysis of cells. Clin Chem 23:1492–1498, 1977.
14. Leif RC: Buoyant density separation and centrifugal cytology analysis of cells. In: Methods of Cell Separation, Catsimpoolas N (ed). Plenum Press, New York, 1979, Vol 2, pp 181–270.
15. Mel HC, Yee JP: Erythrocyte size and deformability studies by resistive pulse spectroscopy. Blood Cells 1:391–399, 1975.
16. Piomelli S, Lurinsky G, and Wasserman LR: The mechanism of red cell aging. I. The relationship between cell age and specific gravity—evaluated by ultracentrifugation in a discontinuous density gradient. J Lab Clin Med 69:659–674, 1967.
17. Rennie CM, Thompson S, Parker AC, Maddy A: Human erythrocyte fractionation in "Percoll" density gradients. Clin Chim Acta 98:119–125, 1979.
18. Schmid-Schonbein H, Gaehtgens P: What is red cell deformability? Scand J Clin Lab Invest 41(Suppl 156): 13–26, 1981.
19. Zucker RM, Wu ND, Mitrani A, Silverman M: Cell volume decrease during Friend leukemia cell differentiation. J Histochem Cytochem 27:413–416, 1979.